Adaptive Multigrid Solutions of Thin Film Flows over Topography

Y.C. Lee[1], H.M. Thompson[2], and P.H. Gaskell[3]

[1] The University of Leeds, LS2 9JT, Leeds, U.K. y.c.lee@leeds.ac.uk
[2] The University of Leeds, LS2 9JT, Leeds, U.K. h.m.thompson@leeds.ac.uk
[3] The University of Leeds, LS2 9JT, Leeds, U.K. p.h.gaskell@leeds.ac.uk

1 Introduction

The behaviour of thin liquid films whether forced to spread or deposited as a distinct pattern on the surface of a substrate, is of enormous significance to many manufacturing and biological processes. The topic of the present study is the flow of continuous thin liquid films over surfaces containing topographical features. In the electronics sector (displays, printed circuits, micro-devices, sensors etc), for example, the industrial goal is often to minimise free surface deviations from planarity either for aesthetic reasons or to ensure predictable product properties [1].

These three-dimensional flows present extremely challenging practical design problems since free surface disturbances caused by even small-scale topography can persist over length scales several orders of magnitude greater than the actual size of the topography. The focus here is on the numerical modelling of such flows, an area which is still in its infancy. The majority of previous numerical studies have modelled the flow using the long wave, lubrication approximation which reduces the three-dimensional Navier-Stokes equations to more tractable two-dimensional fourth order partial differential equations for film thickness, pressure and (for evaporative flow) solvent concentration. Most have solved the resultant time-dependent lubrication equations with alternating-direction implicit (ADI) algorithms using alternating sweeps in each direction so that only a banded system of equations needs to be solved at each time step [2].

Recently, however, a Multigrid approach with adaptive time-stepping has been developed as a more efficient alternative to ADI schemes, having already been applied successfully to droplet spreading flows [3] and continuous film flow with [4] or without evaporation [5]. This paper highlights the additional benefits of adopting an automatic local grid refinement procedure within the Multigrid algorithm which allows fine grids to be used only where they are needed, i.e. near the topographies themselves, and much coarser grids to be used over the rest of the substrate. Several previous numerical studies have

successfully used mesh adaptivity in a wide variety of different contexts [6,7]. Here, the adaptive grid refinement strategy employed lies within the multilevel adaptive technique (MLAT) of Brandt [8]. This approach is readily applicable to the existing Multigrid solver and facilitates grid adaption using local truncation error estimates coupled within the overall Full Approximation Storage (FAS) Multigrid method.

2 Problem Specification and Mathematical Formulation

Figure 1 shows a sketch of the motion of a thin liquid film of thickness $H(X,Y)$ over a flat substrate, containing a small circular trench topography inclined at an angle θ to the horizontal, with a constant volumetric flow Q_0 per unit width. The liquid is assumed Newtonian and incompressible, with constant

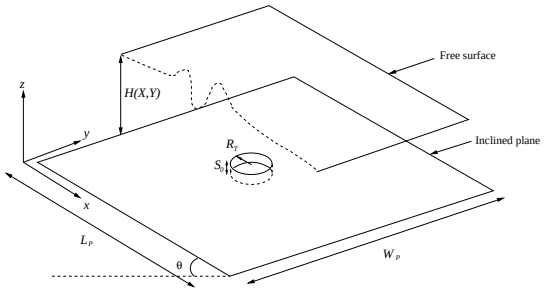

Fig. 1. Gravity-driven thin film flow over a small circular trench.

density ρ, viscosity μ and surface tension σ, and its motion governed by the Navier-Stokes and continuity equations, viz:

$$\rho\left(\frac{\partial \underline{U}}{\partial T} + \underline{U}.\nabla\underline{U}\right) = -\nabla P + \mu\,\nabla^2\underline{U} + \rho\,\underline{g}, \tag{1}$$

$$\nabla.\underline{U} = 0, \tag{2}$$

where $\underline{U} = (U,V,W)$ and P are the fluid velocity and pressure respectively, T is time and $\underline{g} = g(\sin\theta, 0, -\cos\theta)$ is the acceleration due to gravity.

Assuming that $\epsilon = H_0/L_0$ is small, where H_0 and L_0 are the characteristic film thickness and in-plane length scale respectively, yields the following lubrication equation for non-dimensional film thickness h,

$$\frac{\partial h}{\partial t} = \frac{\partial}{\partial x}\left[\frac{h^3}{3}\left(\frac{\partial p}{\partial x} - 2\right)\right] + \frac{\partial}{\partial y}\left[\frac{h^3}{3}\left(\frac{\partial p}{\partial y}\right)\right], \tag{3}$$

and pressure, p:

$$p = -\frac{6}{\beta^3}\nabla^2(h+s) + \frac{2}{\beta}6^{1/3}N(h+s)\ , \tag{4}$$

where $L_0 = \beta\left(\frac{\sigma H_0}{3\rho g \sin\theta}\right)^{1/3}$ and N measures the influence of gravity on free surface shape. Topographies are defined via arctangent functions which enable the steepness of their sides to be controlled easily and the boundary conditions are that the flow is fully developed upstream and downstream. Further details are given in [4].

3 Numerical Method

3.1 Spatial Discretisation

The lubrication equations (3) and (4) are solved on a square computational domain, $(x,y) \in \Omega = (0,1)\times(0,1)$, with equal, uniform grid spacings in the x and y directions, Δ say, leading to the following discretised equations:

$$\begin{aligned}\frac{\partial h_{i,j}}{\partial t} = \frac{1}{\Delta^2}\Bigg[&\frac{h^3}{3}|_{i+\frac{1}{2},j}\,(p_{i+1,j}-p_{i,j}) - \frac{h^3}{3}|_{i-\frac{1}{2},j}\,(p_{i,j}-p_{i-1,j}) + \\ &\frac{h^3}{3}|_{i,j+\frac{1}{2}}\,(p_{i,j+1}-p_{i,j}) - \frac{h^3}{3}|_{i,j-\frac{1}{2}}\,(p_{i,j}-p_{i,j-1})\Bigg] - \\ &\frac{2}{\Delta}\left(\frac{h^3}{3}|_{i+\frac{1}{2},j} - \frac{h^3}{3}|_{i-\frac{1}{2},j}\right),\end{aligned} \tag{5}$$

$$\begin{aligned}&p_{i,j} + \frac{6}{\Delta^2}\Bigg[(h_{i+1,j}+s_{i+1,j}) + (h_{i-1,j}+s_{i-1,j}) + (h_{i,j+1}+s_{i,j+1}) + \\ &(h_{i,j-1}+s_{i,j-1}) - 4(h_{i,j}+s_{i,j})\Bigg] - 2\sqrt[3]{6}N(h_{i,j}+s_{i,j}) = 0,\end{aligned} \tag{6}$$

for each, (i,j), in the computational domain. The terms, $\frac{h^3}{3}|_{i\pm\frac{1}{2},j}$, $\frac{h^3}{3}|_{i,j\pm\frac{1}{2}}$ are the pre-factors obtained from linear interpolation between neighbouring vertices. Time integration is performed using the standard, second-order accurate Crank-Nicholson method and writing the right hand side of equation (5) as $F(h_{i,j}, p_{i,j}, h_{i\pm1,j}, p_{i\pm1,j}, h_{i,j\pm1}, p_{i,j\pm1})$ leads to the equation

$$\begin{aligned}&h_{i,j}^{n+1} - \frac{\Delta t^{n+1}}{2}F(h_{i,j}^{n+1}, p_{i,j}^{n+1}, h_{i\pm1,j}^{n+1}, p_{i\pm1,j}^{n+1}, h_{i,j\pm1}^{n+1}, p_{i,j\pm1}^{n+1}) \\ &= h_{i,j}^{n} + \frac{\Delta t^{n+1}}{2}F(h_{i,j}^{n}, p_{i,j}^{n}, h_{i\pm1,j}^{n}, p_{i\pm1,j}^{n}, h_{i,j\pm1}^{n}, p_{i,j\pm1}^{n}),\end{aligned} \tag{7}$$

for which $\Delta t^{n+1} = t^{n+1} - t^n$, and the right hand sides are given in terms of known values at the end if the nth time step, $t = t^n$.

3.2 Adaptive Multigrid Solution Strategy

Equations (6) and (7) and are solved using a Full Approximation Storage Multigrid algorithm within a Full Multigrid Cycle. Error reduction is performed using a fixed number of pre- and post- Red-Black Gauss-Seidel Newton relaxations. On the coarsest grid level, the discretised equations are solved using Newton iteration. Adaptive local mesh refinement is implemented using the Multi-Level Adaptive Technique (MLAT) first proposed by Brandt [8]. The τ-indicator is used to quantify errors since information is readily available from the different grid levels. The difference in truncation error on successive grids $\mathcal{G}_k$ and $\mathcal{G}_{k-1}$ is approximated via a relative truncation error quantity, τ_k^{k-1}, with large values of τ_k^{k-1} indicating regions of significant error between successive grid levels and where correspondingly further grid refinement is necessary.

A general approach to the discretisation at local refinement interfaces is to conserve numerical flux at both the coarse and fine locally refined regions, where the numerical flux across a control volume is defined via;

$$F = \int\int_S \underline{u} \cdot \underline{n}\, dS \ . \tag{8}$$

For equation (7)

$$\underline{u} = \underline{u}_h = \left(\frac{h^3}{3} \left(\frac{\partial p}{\partial x} - 2 \right), \frac{h^3}{3} \left(\frac{\partial p}{\partial y} \right) \right), \tag{9}$$

and for equation (6)

$$\underline{u} = \underline{u}_p = -\frac{6}{\beta^3} \nabla (h + s) \ . \tag{10}$$

Further details of the adaptive approach used here are given in [9].

4 Results

The cases considered here are for the flow of thin water films of asymptotic film thickness $H_0 = 100\mu m$, viscosity 0.001Pa s, density $\rho = 1000\mathrm{kg\,m^{-3}}$ and surface tension $\sigma = 0.07\mathrm{N\,m^{-1}}$ down a substrate inclined at 30° to the horizontal and with a constant inlet flow rate $Q_0 = 1.635 \times 10^{-6}\mathrm{m^2 s^{-1}}$ [1]. These parameters yield a Capillary length $L_c = 0.78$mm and $N = 0.122$, the latter value indicating that gravity has little influence on the free surface shape. All results are obtained using an FMG V(4,2) cycle with a coarse grid with 9x9 nodes in each direction and finest grid levels up to 513x513 ($k = 6$).

Figure 2 illustrates the flexibility of the adaptive approach by solving flow over a square 39mm x 39mm domain containing three trenches each of characteristic length 3.9mm, depth 10μm and with square, circular and a diamond

cross-sectional shapes indicated on the right hand plan view of the computational grids. The left hand side of the Figure shows the resultant free surface disturbances, with the characteristic upstream capillary ridge and downstream bow wave evident around each isolated topography [4]. It also clearly shows

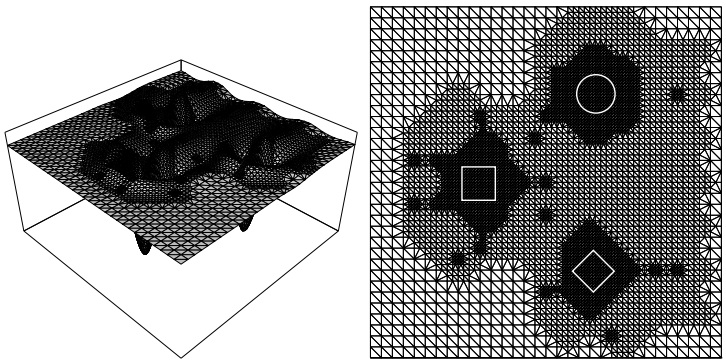

Fig. 2. Flow past three small topographies.

that the greatest refinement is concentrated around the topographies themselves while allowing coarser 33x33 grids to be employed in the simple regions of the flow with the smallest free surface disturbances. The efficiency of the adaptive approach is highlighted for flow past a square trench of dimensions 0.78mm x 0.78mm x 10μm. Figure 3 shows the CPU time for (a single time step?) needed for the adaptive Multigrid solver compared to that taken by the non-adaptive solver. The grid levels used are $k = 2$ (33x33 nodes in each direction), $k = 3$ (65x65),..., $k = 6$ (513x513) over a square 39mm x 39mm substrate. Non-adaptive solutions are calculated on uniformly-spaced grids whereas the adaptive ones use a global coarse 33x33 grid and refine adaptively if the residuals of the discretised equations on grid k are greater than $0.1\tau_k^{k-1}$. Figure 3 shows that the adaptive solutions are much more efficient than the non-adaptive ones. For the case of a 513x513 grid ($k = 6$), for example, the adaptive solution calculates a solution of equal accuracy in less than 10% of the CPU time.

5 Conclusion

Thin film and spreading flows over topographically heterogeneous substrates are of enormous significance in a variety of biological, scientific and industrial processes. A new Multigrid strategy with automatic mesh adaption for investigating thin film flows over arbitrary topography (peaks, trenches and their combination) is introduced which offers substantial efficiency gains compared

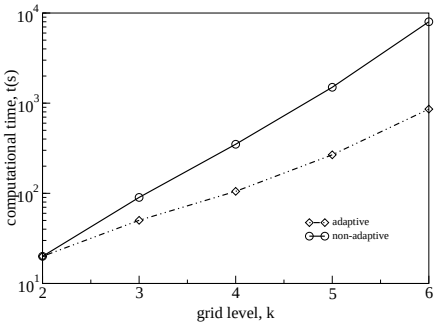

Fig. 3. Comparison between CPU times for adaptive and non-adaptive solution of flow past a square trench.

to the non-adaptive approach. This offers the ability to create fine meshes only in regions exhibiting large gradients in the free surface while allowing coarser meshes to be used in the simpler flow regions.

The adaptive solver is an important development toward the production of practically useful simulation tools that can solve real problems, for example identifying the optimum secondary topography distribution or localised heating sources needed as part of a manufacturing process to planarise free surface flows over desirable topography [1].

References

1. Decre, M.J., Baret, J,C.: Gravity driven flows of viscous liquids over two-dimensional topographies. J. Fluid Mech., **487**, 147–166 (2003).
2. Schwartz, L.W., Eley, R.R.: Simulation of droplet motion on low energy and heterogeneous surfaces. J. Coll. Int. Sci., **202**, 173–188 (1998).
3. Gaskell, P.H., Jimack, P.K., Sellier, M., Thompson, H.M.: Efficient and accurate time adaptive multigrid simulations of droplet spreading. Int J. Numer. Meth. Fluids, **45**, 1161–1186 (2004).
4. Gaskell, P.H., Jimack, P.K., Sellier, M., Thompson, H.M., Wilson, M.C.T.: Gravity-driven flow of continuous thin liquid films on non-porous substrates with topography. J. Fluid Mech., **509**, 253–280 (2004).
5. Gaskell, P.H., Jimack, P.K., Sellier, M., Thompson, H.M.: Flow of evaporating, gravity-driven thin liquid films over topography. Phys. Fluids, **18**, 031601 (2006).
6. Bai, D., Brandt, A.: Local Mesh Refinement Multilevel Techniques. SIAM J. Sci. Stat. Comput., **8(2)**, 109–134 (1987).
7. Trangenstein, J.A., Kim, C.: Operator Splitting and Adaptive Mesh Refinement for the Luo-Rudy I Model. J. Comput. Phy., **196**, 645–79 (2004).
8. Brandt, A.: Multi-Level Adaptive Solutions to Boundary-Value Problems. Math. Comp., **31**, 333–90 (1977).
9. Lee, Y.C., Thompson, H.M., Gaskell, P.H.: An efficient adaptive multigrid algorithm for predicting thin film flow on surfaces containing localised topographic features. Computer and Fluids, to appear (2006).